The Egyptian Journal of Radiology and Nuclear Medicine (2016) 47, 969–984

Egyptian Society of Radiology and Nuclear Medicine

The Egyptian Journal of Radiology and Nuclear Medicine

www.elsevier.com/locate/ejrnm
www.sciencedirect.com

ORIGINAL ARTICLE

Role of conventional MRI and MR arthrography in evaluating shoulder joint capsulolabral-ligamentous injuries in athletic versus non-athletic population

Nevien El-Liethy *, **Heba Kamal, Rania F. Elsayed**

Lecturer at Radiology Department, Cairo University, Egypt

Received 16 March 2016; accepted 4 May 2016
Available online 16 June 2016

KEYWORDS

MRI;
MRA;
Capsulo;
Labral injury;
Athletes

Abstract *Objective:* The aim of this study was to assess diagnostic value of direct MR arthrography compared to conventional MR imaging in the diagnosis of different pathologic entities affecting the capsule-labral complex in athletic and non-athletic population.
Subjects and methods: This study included 60 patients complaining of shoulder pain. Conventional MRI and MR arthrography (MRA) were done for all cases. The musculoskeletal radiologist reviewed the images for evidence of pathologies of the labroligamentous complex. Inter-observer agreement was determined with kappa statistics, and the diagnostic accuracy of each technique was calculated.
Results: Comparing the sensitivity of conventional MRI versus MRA was done by correlating the final diagnosis of each modality with the results of arthroscopy. MRI revealed sensitivity (SEN) of 72%, specificity (SPE) of 78%, while MRA revealed a SEN of 78%, SPE of 100%, PPV of 100%, and NPV of 21%.
Conclusion: MR techniques cannot replace arthroscopy; however, they could be a potent additional tool for diagnosis of the main pathological affection of the shoulder joint guided by the type of the population, which proved to have good impact on the diagnosis. The capsulolabral and ligamentous injuries are more common at the athletic group while the non-athletic population are more prone to rotator cuff tendons injury.

1. Introduction

In the last decade, understanding the biomechanics and physiology of the athletic shoulder and of shoulder-stabilizing forces has significantly improved. It is now understood that instability related to sports activities is associated with secondary impingement, muscular dysfunction, and damage to intra-articular structures that can be detrimental to athletes'

* Corresponding author.
E-mail addresses: nevienelliethy@yahoo.com (N. El-Liethy), hebakamala@yahoo.com (H. Kamal), rania729@hotmail.com (R.F. Elsayed).
Peer review under responsibility of The Egyptian Society of Radiology and Nuclear Medicine.

http://dx.doi.org/10.1016/j.ejrnm.2016.05.001
0378-603X

performance and ultimately to their careers. For athletes, glenohumeral instability is recognized as an important cause of ongoing shoulder pain and dysfunction. The high degree of mobility of the shoulder joint makes it inherently prone to capsule-labral or ligamentous injuries. Repetitive throwing action places high stress loads on the capsulo-labral complex and rotator cuff (1).

MR imaging of the glenohumeral joint for evaluation of labrum or capsular tears is a challenging task for most musculoskeletal radiologist. A number of investigators have reported, with varied results, on the accuracy of conventional MR imaging of the glenoid labrum. The complexity of the capsulolabral anatomy and the subtlety of the MR imaging findings necessitate knowledge of anatomic details and experience on the part of radiologist to achieve acceptable results (2).

MR arthrography extends the capabilities of conventional MR imaging because contrast solution distends the joint capsule, outlines intra-articular structures, and leaks into abnormalities. It exploits the natural advantages gained from joint effusion. Either saline solution or diluted gadolinium may be injected as the MR arthrographic contrast material (3).

1.1. The aim of this study

To assess the diagnostic value of direct MR arthrography compared to conventional MR imaging in the diagnosis of different pathologic entities affecting the capsulolabral and ligamentous complex in athletic patients compared to the non-athletic patients.

2. Patients and methods

Sixty patients, complaining of history of trauma, pain (acute or chronic) and/or dislocation (voluntary, involuntary, recurrent or once), with age range from 14 to 55 years (mean age 35 years), referred to the Radiology Department, Faculty of Medicine kasr El-Eini, Cairo University from the outpatient clinic of the Orthopedic Department between June 2015 and December 2015. Approval consent was taken from all patients before doing this study. This study was approved by the Ethics Committee of Cairo University. All patients were subjected to history taking, clinical provisional diagnosis, conventional MRI, MR Arthrography and arthroscopy.

They were subdivided into two groups: athletic and non-athletic.

2.1. Magnetic resonance imaging

Devices: GYROSCAN INTERNA 1.5T MAGNET (PHILIPS) or SYMPHONY 1.5T MAGNET (SIEMENS).

Patient position: The patient laid in supine position with the head directed toward the scanner bore. The used position of the patient's arm is neutral to slightly externally rotate. Surface coil (flexible coils).

Imaging planes (Fig. 1) and pulse sequences

- Preliminary Scout Localizer in axial, sagittal, coronal.
- Coronal oblique T1 (TSE, TR 664, TE 18, FOV 14, SL 4, MTARIX 205/512, NSA 3).
- Coronal oblique T2 (TSE, TR 2411, TE 100, FOV 14, SL 4, MTARIX 201/512, NSA 2).
- Coronal oblique STIR (TSE, TR 2411, TE 15, FOV 14, SL 4, MTARIX 201/512, NSA 2).
- Coronal oblique PD (TSE, TR 1400, TE 16, FOV 18, SL 4, MTARIX 201/512, NSA 3).
- Axial GR (TSE, TR 551, TE 18, FOV 17, SL 4, MTARIX 179/512, NSA 3).
- Sagittal oblique T2 (TSE, TR 3342, TE 100, FOV 16, SL 4, MTARIX 205/512, NSA 3).

2.2. Magnetic resonance arthrography

2.2.1. Technique (Fig. 2)

The area is prepared and draped in a sterile fashion. The subcutaneous tissue is anesthetized.

A lead marker is placed under fluoroscopic guidance just lateral to the junction between middle and lower third of the medial cortex of the humeral head.

The needle tip (22-gauge) is advanced in an anteroposterior direction perpendicular to the fluoroscopic beam until it reaches the humeral head.

The needle is angled obliquely toward the glenoid. Start injection of the contrast (the mixture used is composed of 0.1 ml gadopentetate dimeglumine, 5 ml non-ionic contrast, 3 ml xylocaine and completed to 20 ml with sterile saline). To confirm intra-articular placement of contrast material, one must observe a column of contrast agent between the glenoid and the humerus.

2.2.2. MRA protocol

The patient should be scanned with MRI during max. 30 min of injection, the same surface coil is used and all pulse sequences are done with T1 fat suppression (TR 924, TE 17, FOV 15, NEX 3) in axial, coronal and sagittal planes.

2.3. Analysis of MRI and MRA images

Two radiologists, with experience in musculoskeletal radiology respectively, independently performed MRI and MRI analyses in a randomized blind fashion. Analysis was performed on a PACS workstation.

Classic bankart lesion (Figs. 3 and 4) was manifesting as tear of the anterior inferior labrum with associated periosteal tear. Bankart lesion is usually accompanied by Hill-Sachs lesion.

ALPSA lesion (Figs. 9–11) was defined as an avulsion and medial rolling of the inferior labroligamentous complex along the scapular neck. The main differentiating point of ALPSA from a Perthes lesion is the displacement of the torn labroligamentous tissue, which is undisplaced or shows minimal displacement in Perthes lesion. An ALPSA lesion differs from a Bankart lesion in that an ALPSA lesion has an intact anterior scapular periosteum (it is ruptured in Bankart lesion) that allows the labroligamentous structures to displace medially and rotate inferiorly on the scapular neck.

Perthes lesion (Figs. 12 and 13) was defined as a tear of the glenoid labrum with intact scapular periosteum. The torn anterior labrum is often undisplaced and visualized in its normal location on conventional MR imaging.

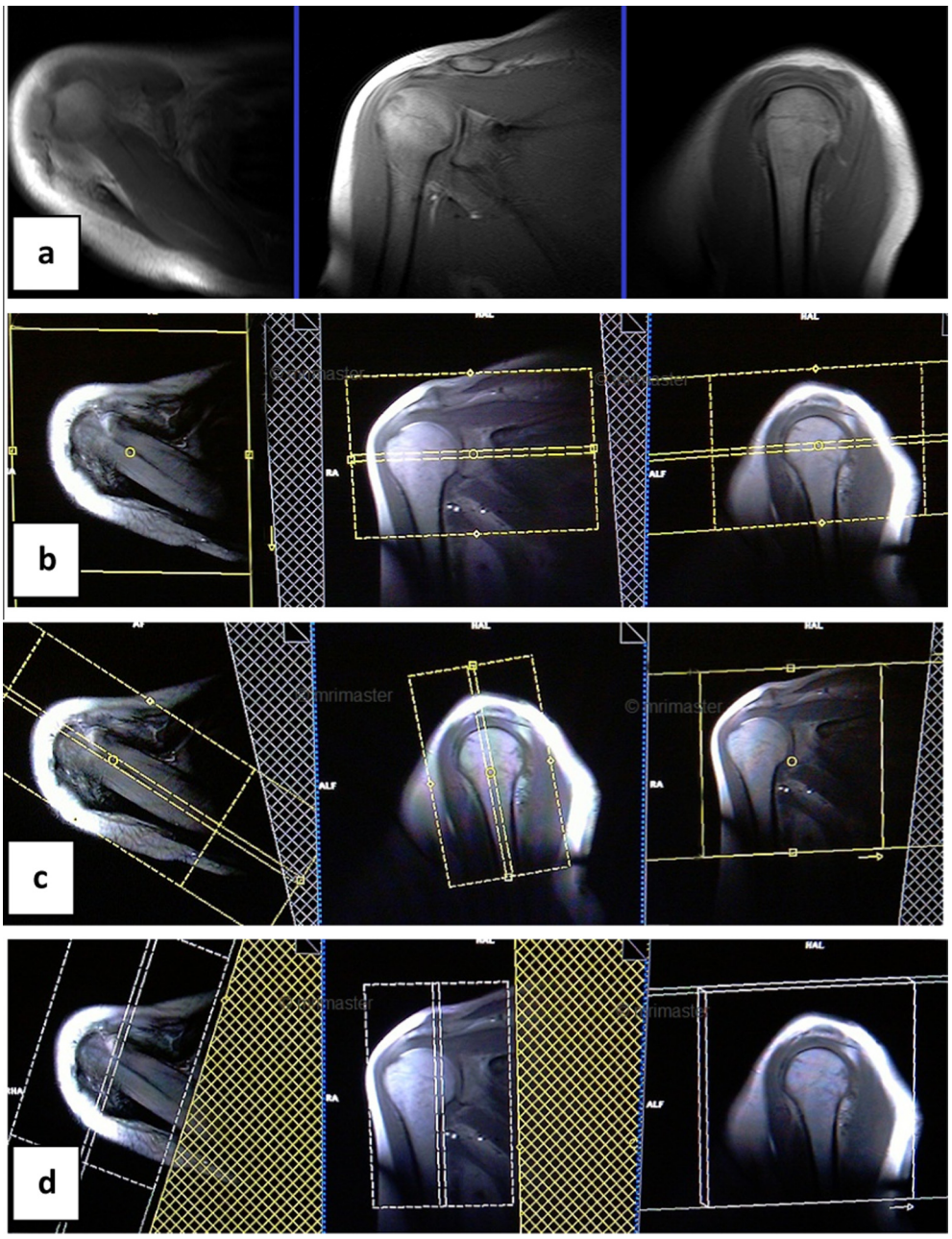

Fig. 1 (a–d) Showing imaging localizer (a) and planes axial (b), coronal (c) and sagittal (d) (21).

GLAD lesion (Figs. 18 and 19) showed a superficial anterior inferior labral tear associated with an anterior inferior articular cartilage injury. The use of intra-articular contrast in MR arthrogram helps to visualize the small tears at the level of the anterior inferior glenoid rim.

SLAP type II (Fig. 11) was diagnosed by MRA where an injury involving the superior aspect of the glenoid labrum includes the biceps tendon anchor. In type II, Labrum and biceps anchor point detached from superior rim of glenoid.

Reversed Bankart lesion (Fig. 15) shows Detachment of the postero-inferior labrum (6–9 o'clock) with tearing of the posterior scapular periosteum.

Rotator cuff tears (Figs. 5–8, 16 and 17) are seen on imaging as thinning, irregularity or focal discontinuity. MRI has limits in its ability to accurately detect tears, and MR arthrography remains the imaging modality of choice. RCT pathologies can be classified by location (articular, bursal, and intratendinous), the tendons involved (supraspinatus, infraspinatus, teres minor, and subscapularis), and the tears based on location (articular, bursal, and intratendinous).

MDI (multidirectional instability) (Figs. 20 and 21). The rotator interval dimensions were measured on sagittal oblique T1-weighted images with fat saturation on the lateral-most sagittal-oblique cut in which the coracoid process was present. The width of the rotator interval was measured on the sagittal

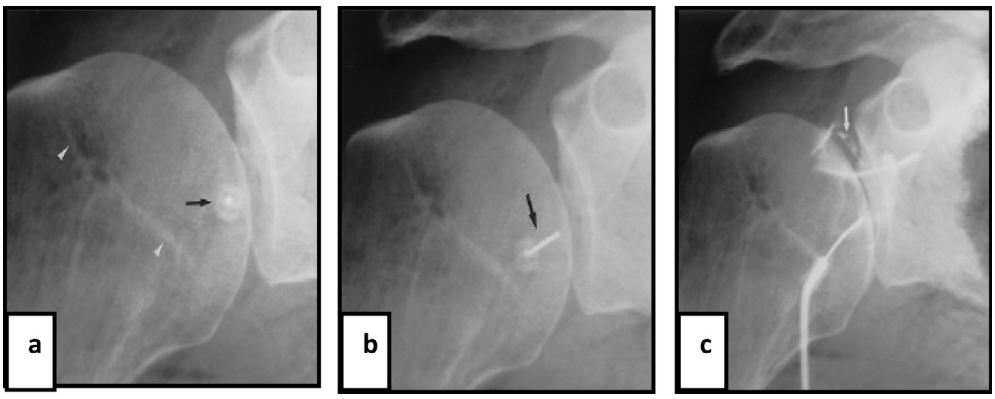

Fig. 2 (a–c) Anterior approach, fluoroscopic guidance for glenohumeral injection. (a) Anteroposterior fluoroscopic image demonstrates a spinal needle (arrow) centered over the needle hub, just lateral to the medial cortex of the humeral head. Note the sclerotic line, which approximates the lateral border of the glenohumeral joint (arrowheads). (b) Anteroposterior fluoroscopic image shows the needle (arrow), which is angled medially toward the glenohumeral joint space after making contact with the humeral head. (c) Anteroposterior fluoroscopic image demonstrates intra-articular contrast material visualized between the glenoid and humerus (arrow) (22).

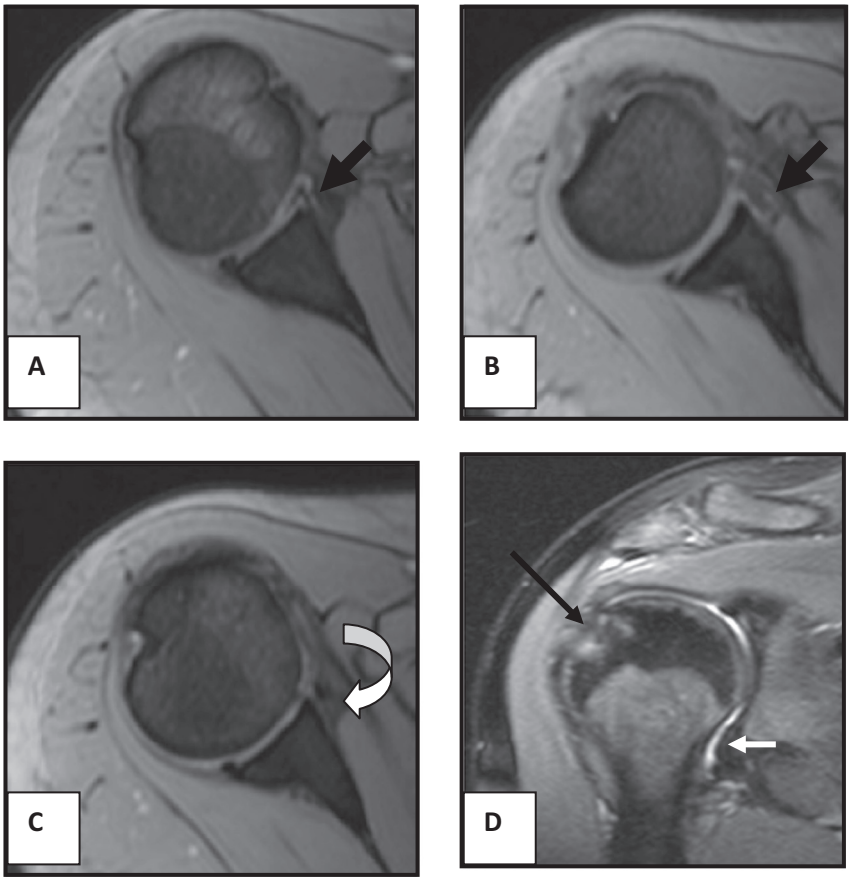

Fig. 3 (A–D) (conventional MRI) showing an athlete Female patient 32 years old complaining of pain after recurrent shoulder joint dislocation; showing Bankart's lesion, Hill Sachs lesion, and joint effusion. (A–C) Axial GR WIs show non-visualized anterior labrum (black arrow) with abnormal signal intensity lesion is seen antero-medial to the scapular body (curved arrow in C). (D) Coronal oblique STIR image shows Hill Sachs lesion (black arrow) eliciting high signal intensity associated with joint effusion (white arrow).

image from the superior border of the subscapularis tendon to the anterior border of the supraspinatus tendon. The depth of the rotator interval was the longest perpendicular distance from the humeral head to the roof of the rotator interval.

The dimensions of the glenohumeral joint capsule were measured on sagittal oblique T1-weighted images with fat saturation en face to the glenoid articular surface. The anteroinferior dimension was the maximal capsular dimension perpendicular to the superior inferior poles line passing through the center of

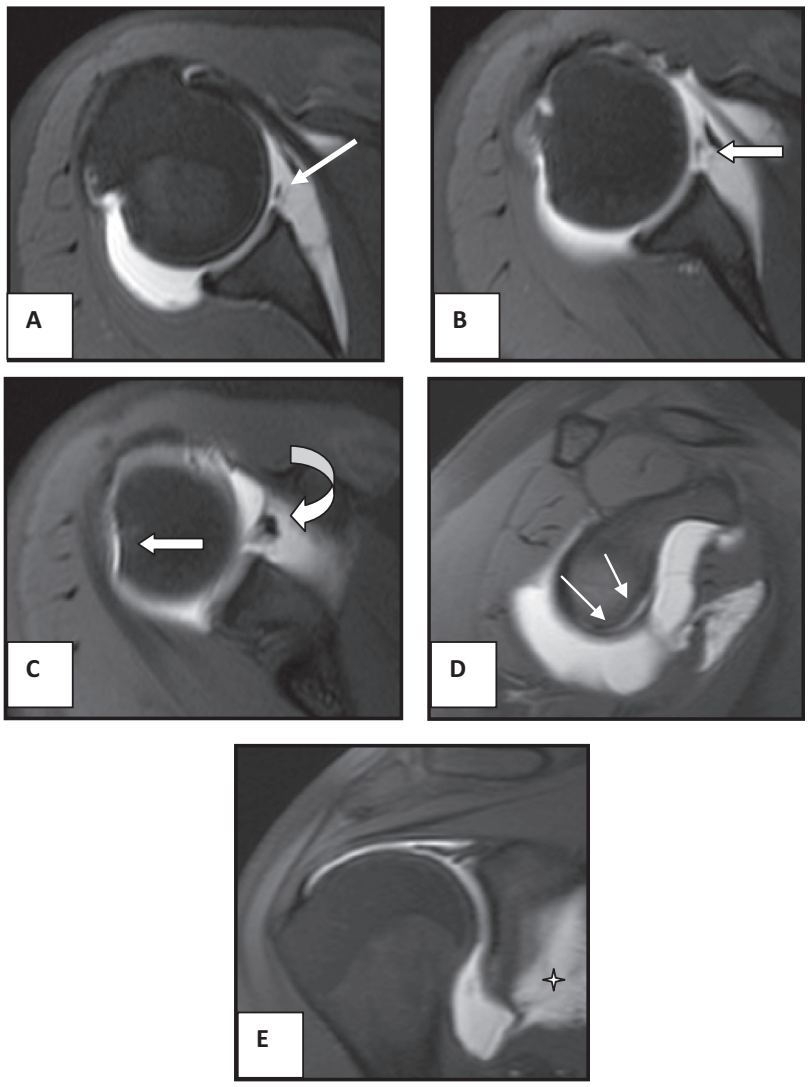

Fig. 4 (A–D) Fat suppressed T1WIs arthrogram images for an athlete Female patient 32 years old complaining of pain after recurrent shoulder joint dislocation showing Bankart's lesion, Hill Sachs lesion, and no supraspinatus tendon tear. In axial plane (A–C) shows completely detached antero-inferior labrum (white arrow in A and B) attached to the inferior glenohumeral ligament (curved arrow in C). Hill Sachs lesion (straight arrow in C). (D) In sagittal oblique confirms antero-inferior labral tear. (E) In coronal oblique shows torn inferior labrum with abnormal configuration of IGHL and leakage of contrast outside (∗).

the glenoid fossa. The posteroinferior dimension was the maximal capsular dimension parallel to this line.

2.3.1. Statistical analysis

Data were statistically described in terms of range, mean, standard deviation (SD), frequencies (number of cases) and percentages when appropriate. Accuracy was represented using the terms sensitivity, specificity, and overall accuracy. All statistical calculations were done using computer programs Microsoft Excel 2003 (Microsoft Corporation, NY, USA) and SPSS (Statistical Package for the Social Science; SPSS Inc., Chicago, IL, USA) version 15 for Microsoft Windows.

Using Chi-Square Tests (Pearson Chi-Square, Likelihood Ratio and Linear-by-Linear Association) P value is considered significant if <0.01 and non-significant if $P > 0.01$.

Accurate statistical analysis of the sex and age of patients, their main complaints as well as the elicited findings with MRI techniques were tabulated.

3. Results

The results are summarized in Tables 1–6.

Classification was done according to whether the patient was athletic or non-athletic and frequency and percentage of labro-ligamentous pathology (Table 1, Chart 1). The former group (35 patients) showed higher incidence of labro-ligamentous injury mainly SLAP while the latter group (25 patients) was more prone to rotator cuff injury rather than labro-ligamentous injury. $P < 0.01$ means significance.

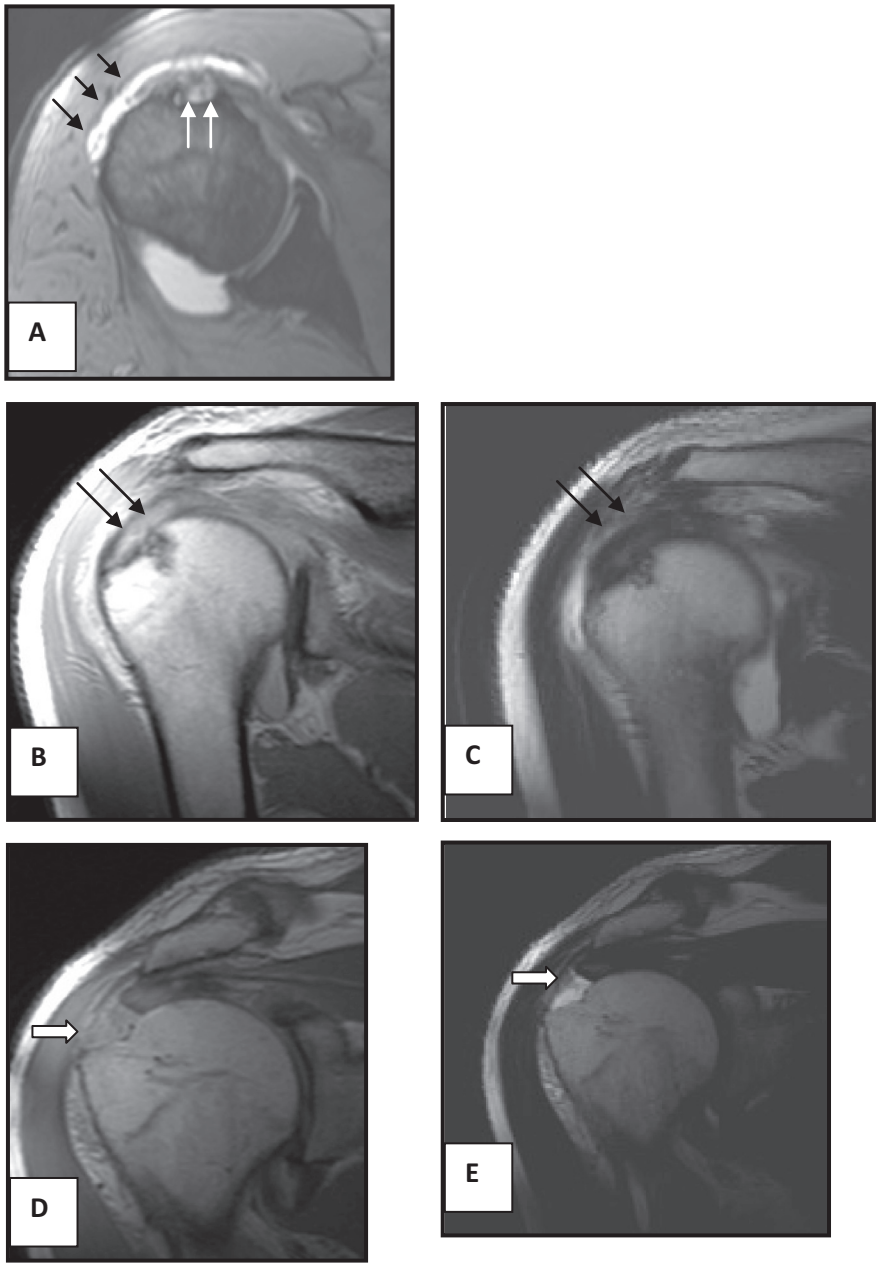

Fig. 5 (A–F) (Conventional MRI[a] images) showing non-athlete male patient 55 years old complaining of pain and limitation of movement of the right shoulder joint after dislocation following acute trauma? Full thickness tear of supraspinatus tendon, intrasubstance tear of infraspinatus tendon, long head of biceps tendon tear, and joint effusion. (A) Axial T1 WI and GR WIs show suspecting tear, joint effusion extending to sub-deltoid bursa (black arrows in B) and non-visualized LHB (double arrow in B) at the bicipital groove. (B and C) Coronal oblique PD & T2 WIs at the level of scapular spine show thick linear high signal intensity within the infraspinatus tendon. (D and E) Coronal Oblique PD & T2 WIs at the level of acromioclavicular joint show full thickness tear of the supraspinatus tendon with a gap seen filled with fluid at its humeral insertion (white arrow).

3.1. Conventional MRI findings: Figs. 3, 5, 9, 12, 14, 16, 18 and 20

The findings are tabulated in Tables 2 and 3 showing the frequency of the pathological lesions involving the antero-inferior and posterior labra as well as the rotator cuff tendons. The superior labrum as well as the capsule could not be assessed in all patients. Other finding as effusion was detected in 9 patients, Hill Sachs lesion was detected in 22 patients and humeral head Subchondral cysts were seen in five patients.

3.2. MR arthrography findings: Fig. 4, 6–8, 10, 11, 13, 15–17, 19, 21 and 22

The arthrographic findings are tabulated in Tables 4 and 5 showing the detailed pathological lesions of the rotator cuff

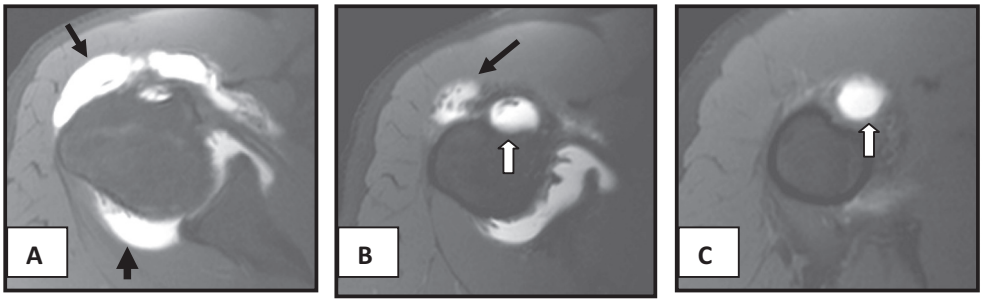

Fig. 6 (A–C) Fat suppressed T1WIs axial arthrogram images show attenuated torn anterior labrum (arrowed in A), non visualized LHB tendon in the bicipital groove (arrowed in B and C) and contrast leakage at the Subdeltoid bursa with multiple loose bodies floating within (black arrow in A and B).

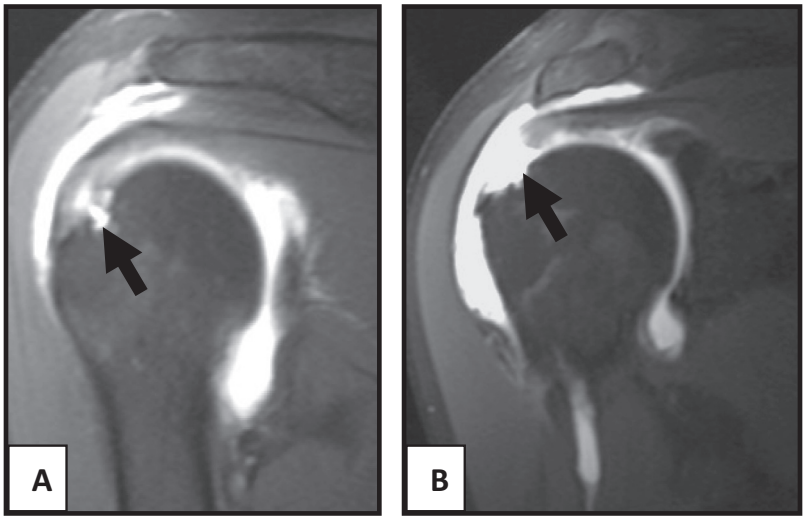

Fig. 7 (A and B) Fat suppressed T1 WIs coronal oblique arthrogram images at the level of scapular spine, (A) showing articular surface tear of infraspinatus tendon & at the level of acromioclavicular joint (arrowed) and (B) showing full thickness tear of supraspinatus tendon with contrast leakage through the gap to fill the sub-deltoid bursa (arrowed).

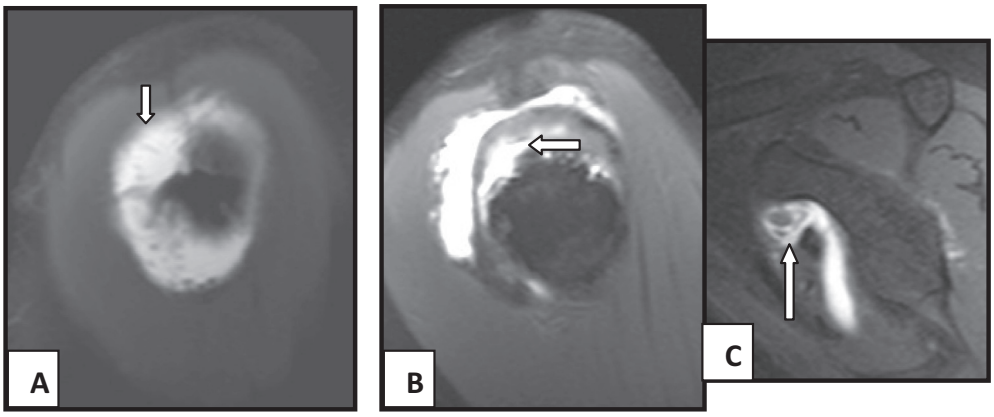

Fig. 8 (A–C) Fat suppressed T1 WIs sagittal oblique arthrogram images confirm full thickness tear of supraspinatus tendon from humeral insertion where contrast leakage seen just beneath the deltoid muscle = arrowed (A), articular surface partial tear of infraspinatus tendon = arrowed (B) and loose body (arrowed) is seen in sub-coracoid bursa (C).

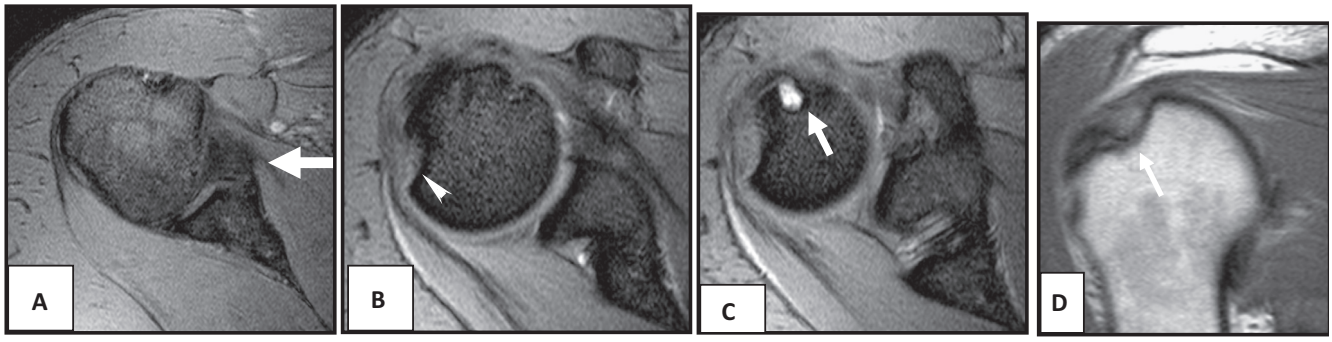

Fig. 9 (A–D) Male patient 30 years old complaining of pain and limitation of movement after right shoulder dislocation following direct trauma. Conventional MRI showing Bankart's lesion with Hill Sachs defect and Subchondral cystic changes. Axial GR images showed lesion of abnormal signal intensity at the anatomical location of anterior labrum (thick arrow) (A), postero-lateral humeral head defect (arrow head) denoting Hill Sachs lesion (B), humeral head subchondral cyst anteriorly (arrow) (C). Coronal T1 image showed Hill Sachs lesion (arrow) (D).

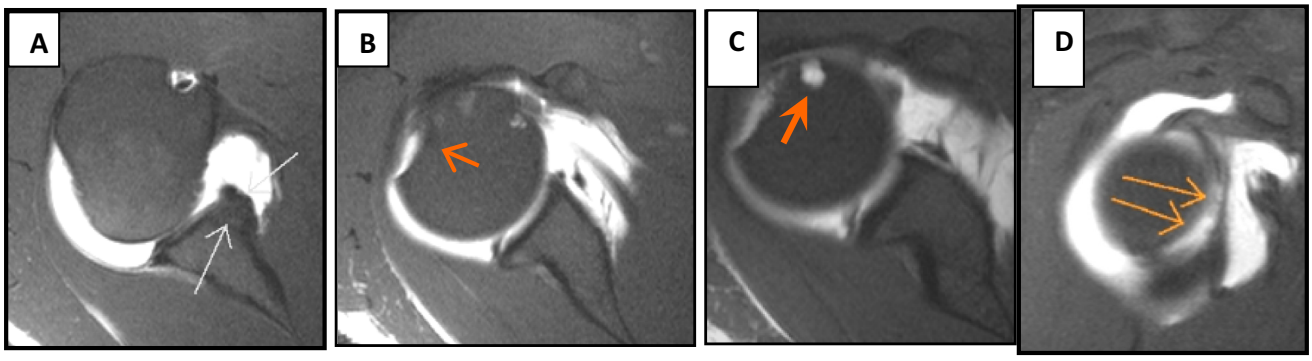

Fig. 10 (A–D) Male patient 30 years old complaining of pain and limitation of movement after right shoulder dislocation following direct trauma. MRA images ALPSA (anterior labro-ligamentous periosteal sleeve avulsion) lesion with Hill Sachs lesion, SLAP II and subchondral cyst: Fat suppressed axial T1 weighted images MR arthrogram showed a globular lesion located medial to the margin of the glenoid (arrowed). No labral tissue is identified at the anterior inferior aspect of the glenoid (A). Hill Sachs deformity (B). Subchondral cyst anteriorly is seen filled with contrast (C). Fat suppressed sagittal oblique T1 weighted images MR arthrogram showed defective antero-inferior labrum (orange arrows) with contrast leakage at its glenoid attachment (D).

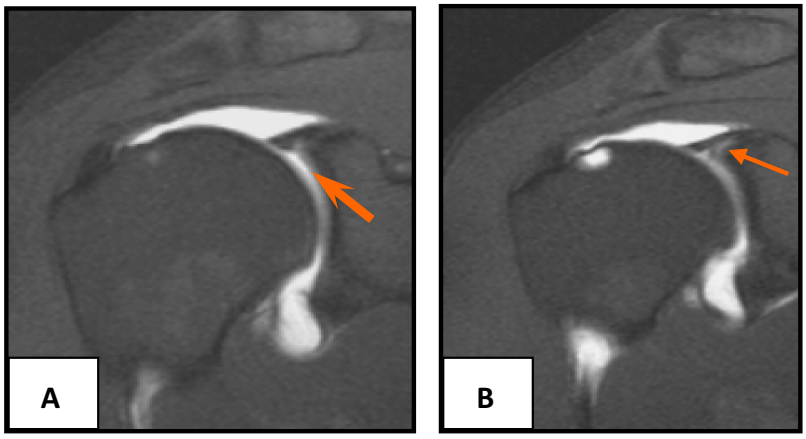

Fig. 11 (A and B) Male patient 30 years old complaining of pain and limitation of movement after right shoulder dislocation following direct trauma MRA images ALPSA (anterior labro-ligamentous periosteal sleeve avulsion) lesion with Hill Sachs lesion, SLAP II and subchondral cyst: Fat suppressed coronal oblique T1 weighted images MR arthrogram showed a linear contrast is seen at the base of the superior labrum (arrowed in A) and insertion of the biceps tendon (arrowed in B).

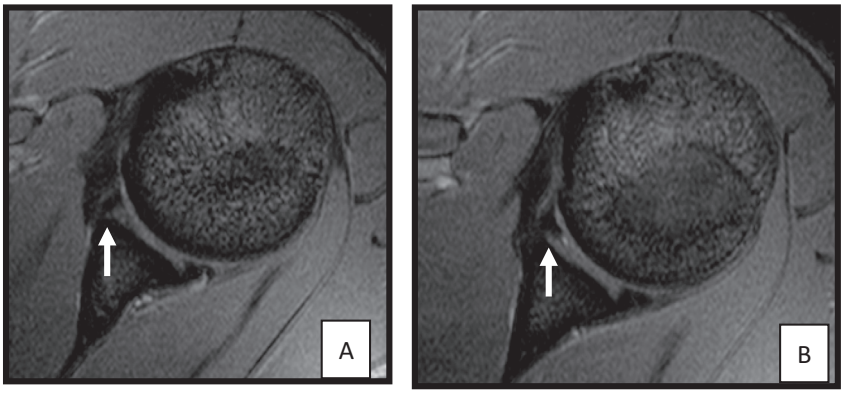

Fig. 12 (A–B) Perthes lesion. An athletic male patient 20 years old, athletes, complaining of pain and recurrent right shoulder dislocation with no history of direct trauma. Axial GR at the level of anterior labrum showing no abnormality detected (white arrow)

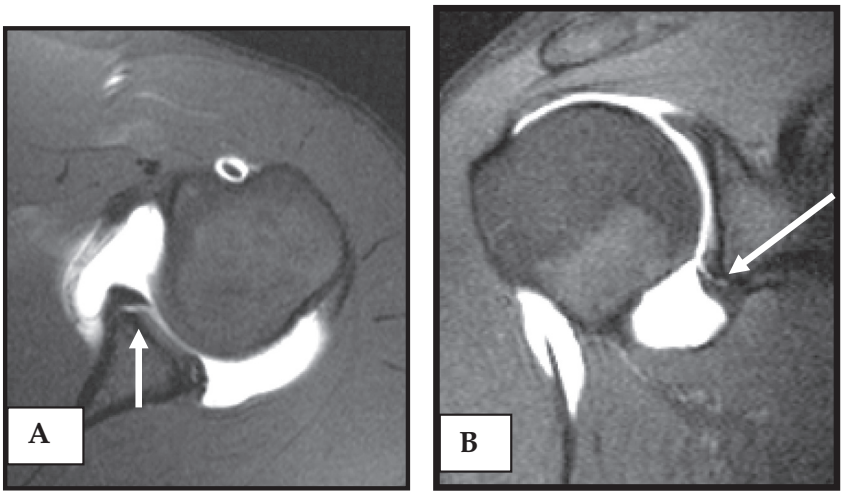

Fig. 13 (A and B) Perthes lesion. An athletic male patient 20 years old, athletes, complaining of pain and recurrent right shoulder dislocation with no history of direct trauma. Fat suppressed axial (A) & coronal (B) T1 weighted images MR arthrogram showed contrast leakage at the base of the detached non-displaced anteroinferior labrum (arrowed).

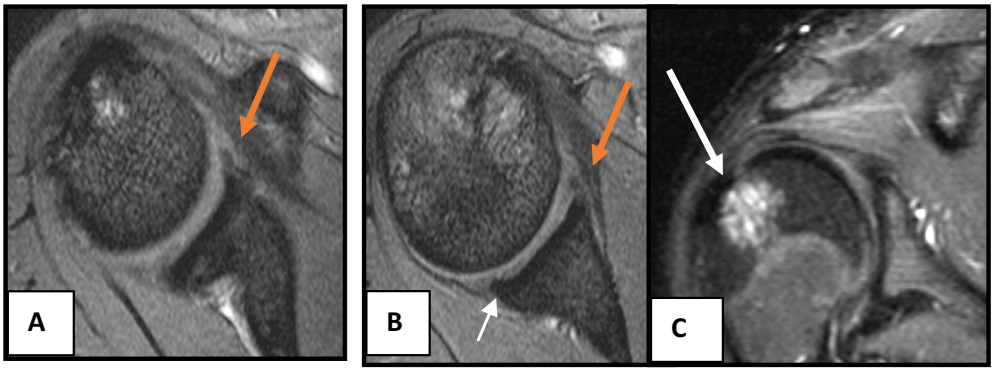

Fig. 14 (A–C) Bankart's lesion and reversed Bankart's lesion. Male patient 21 years, athlete, complaining of pain and limitation of movement after recurrent right shoulder joint dislocation following trauma. Conventional MRI diagnosis was Bankart's lesion with Hill Sachs deformity associated with normal posterior labrum. (A and B) Axial GR weighted images showing abnormal configuration as well as signal intensity of the anterior labrum (orange arrow in A and B). Normal posterior labrum (short white arrow in A). (C) Coronal PD image shows Hill Sachs deformity (long white arrow in C).

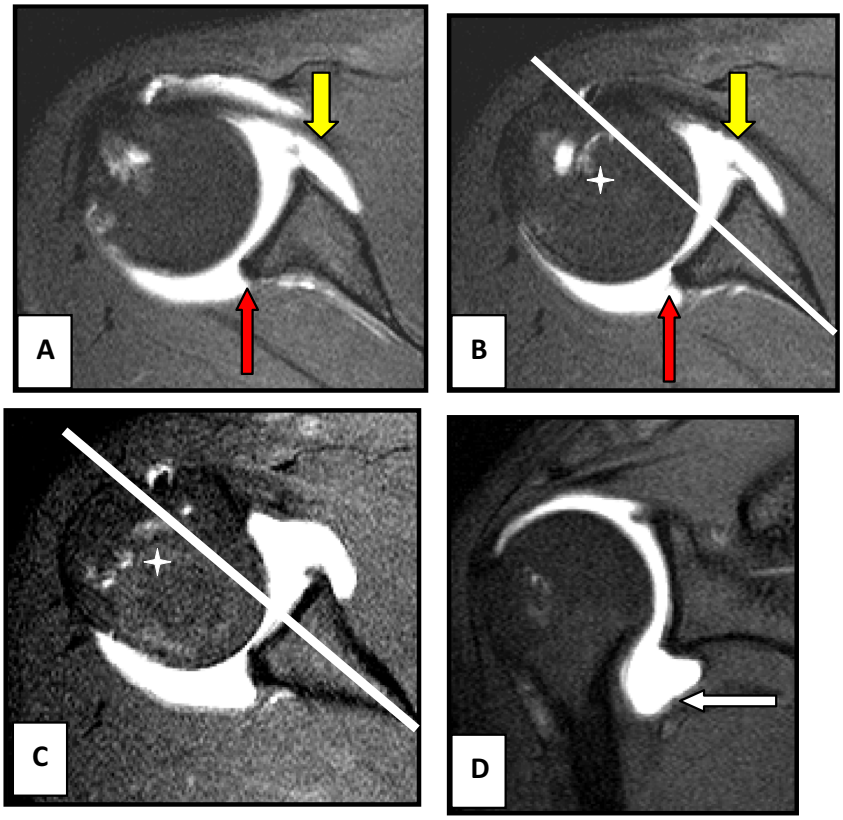

Fig. 15 (A–D) Bankart's lesion and reversed Bankart's lesion. Male patient 21 years, athlete, complaining of pain and limitation of movement after recurrent right shoulder joint dislocation following trauma. Fat suppressed T1WIs arthrogram images showing Bankart's lesion and reversed Bankart's lesion associated with Hill Sachs deformity. (A–C) Fat suppressed T1 WIs MR Arthrogram axial images showing torn posterior labrum (yellow arrows in A and B), torn & detached anterior labrum (red arrows in A and B). The center of humeral head is seen posterior to the scapular line (negative humeral translation) (C). (D) Fat suppressed T1 WI MR Arthrogram coronal image showing torn inferior labrum with abnormal morphology of the axillary recess of IGHL (white arrow head in D).

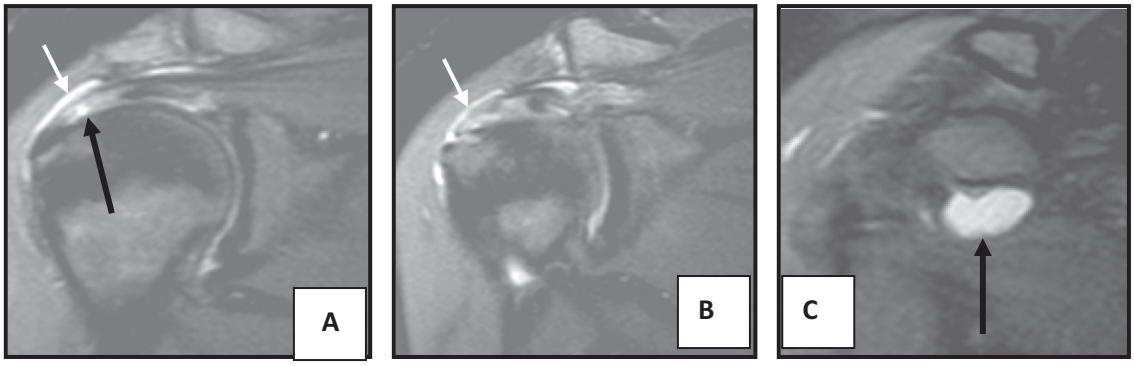

Fig. 16 (A–C) Non-athlete female patient 40 years old complaining of pain and limitation of movement of the right shoulder joint after trauma. Conventional MRI diagnosis was partial tear of the supraspinatus tendon, joint effusion with sub-coracoid bursitis. (A and B) Coronal oblique STIR images show partial tear of the supraspinatus tendon (articular surface), effusion (white arrow). (C) Fluid distending the Subcoracoid bursa denoting bursitis (arrow).

tendons, antero-inferior labrum as well as the posterior labrum.

The type of capsular attachment was seen in 60 patients where type I was seen in 12 patients, type II was seen in 9 patients, type III seen in 7 patients and torn in 32 patients. The superior labrum showed type I SLAP lesion in one patient, and type II in two patients. Hill Sachs defect was detected in 22 patients. Subchondral cysts were seen in five patients. Loose bodies were detected in two patients.

3.3. Comparative statistical analysis (Table 6)

By comparing the capability of MR techniques (MRI and MRA) to achieve accurate diagnoses with that of the arthro-

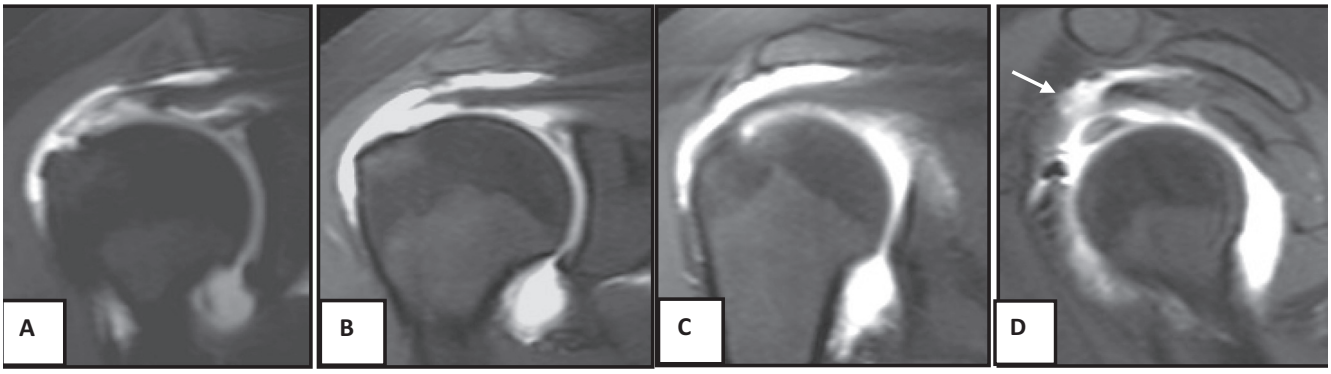

Fig. 17 (A–D) Non-athlete female patient 40 years old complaining of pain and limitation of movement of the right shoulder joint after trauma. Fat suppressed T1WIs (A and B) coronal MR arthrogram images show full thickness tear of the supraspinatus tendon (solid arrows in A and B) with contrast seen leaking to the Subdeltoid bursa (arrow in C and D) associated with linear contrast leakage at the base of the superior labrum denoting SLAP II lesion (hallow arrows in A and B). (D) Fat suppressed T1WIs sagittal oblique MR arthrogram images full thickness tear of supraspinatus tendon and contrast leakage in the subdeltoid bursa (arrow in D).

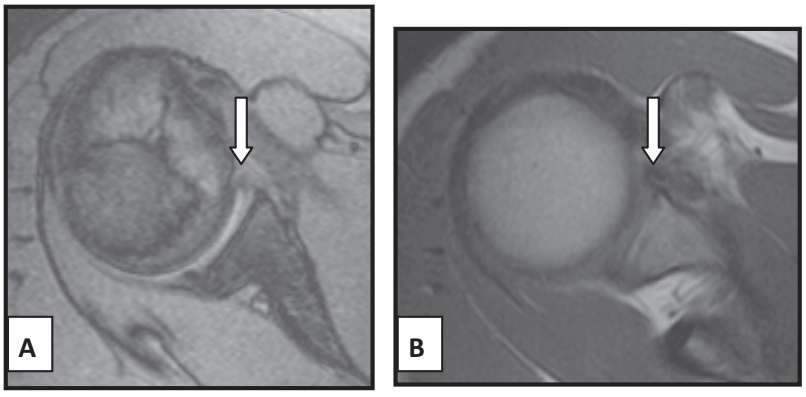

Fig. 18 (A–B) GLAD lesion. Male patient 16 years old, athlete, complaining of anterior shoulder pain after one attack of dislocation. Conventional MRI showing Bankart's lesion: (A) axial GR weighted image (WI), (B) axial T1 WI showed torn anterior labrum which elicited abnormal signal intensity as well as morphology (arrowed in A and B).

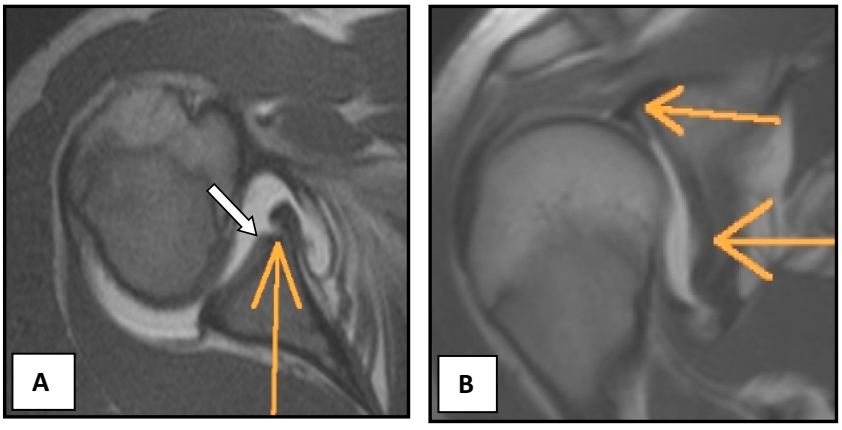

Fig. 19 (A and B) GLAD lesion. Male patient 16 years old, athlete, complaining of anterior shoulder pain after one attack of dislocation. MRA images showing glenolabral articular disruption and SLAP. (A) Transverse T1-weighted MR arthrogram showed a non-displaced tear of the anterior labrum (white arrow) associated with a full-thickness chondral defect of the anterior glenoid (long yellow arrow). (B) Coronal oblique T1-weighted arthrogram showed a contrast leakage below the base of superior labrum (upper yellow arrow) and glenoid chondral defect (lower yellow arrow).

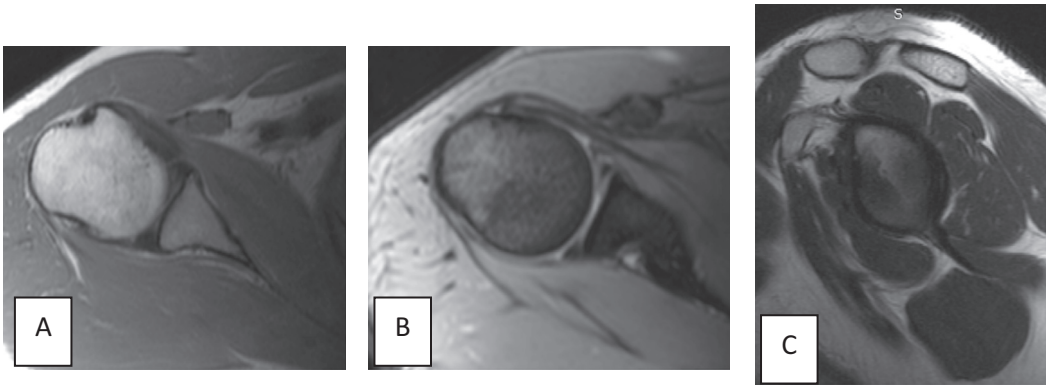

Fig. 20 (A–C) MDI. An athelete female 20 years old complaining of pain during swimming training; showing normal MRI images. (A and B) Transverse T1-weighted and GR-weighted images (C) sagittal T1-weighted image showing no abnormalities could be depicted.

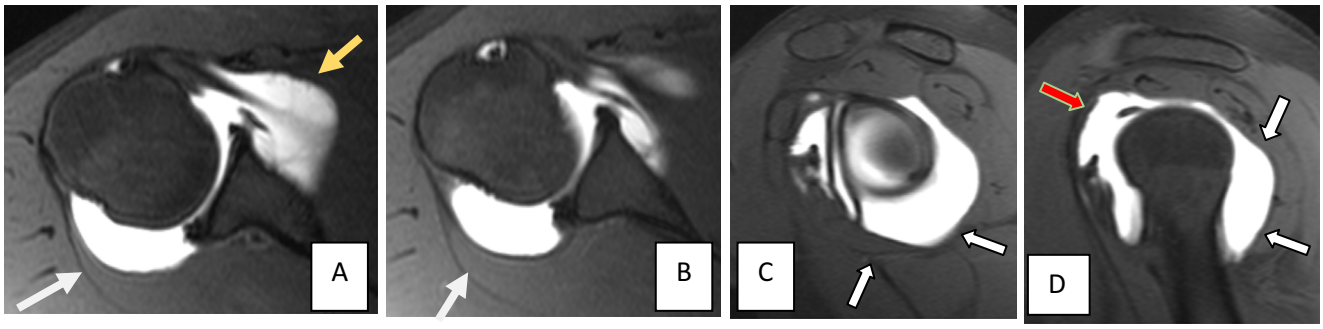

Fig. 21 (A–D) MDI. An athlete female 20 years old complaining of pain during swimming training. MRA images showing MDI finding. (A and B) Transverse T1-weighted MR arthrogram showed capacious posterior capsule (white arrow) associated with wavy anterior capsule (yellow arrow). (C and D) Axial oblique T1-weighted arthrogram showed wavy lobulated posterior capsule (white arrows) and distended anterosuperior capsule (red arrow).

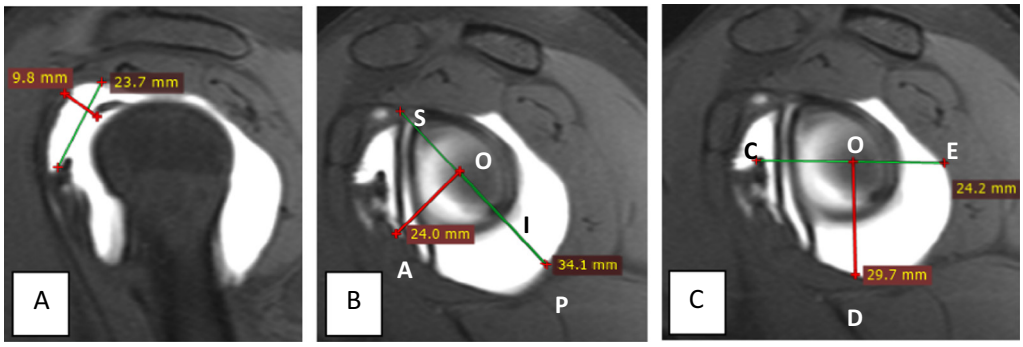

Fig. 22 (A–C) MDI. An athlete female 20 years old complaining of pain during swimming training. MRA images showing MDI findings by using the measurements of the rotator interval as well as capsular distensions. Sagittal oblique T1-weighted MRA images (A) show a redundant rotator interval. The width of the rotator interval is 23.7 mm and the depth is 9.8 mm. (B) The dimensions of glenohumeral joint capsule on sagittal oblique image en face to the glenoid articular surface are 24 mm at the anteroinferior region (OA), 34.1 mm at the at the posteroinferior region (I), and (C) the dimensions of glenohumeral joint capsule on sagittal oblique image 29.7 mm at the inferior region (OD) and 24.2 mm at the posterior region (OE).

scopy, they showed accuracy approximately 97% and high specificity (100%) ($p < 0.001$).

4. Discussion

Magnetic resonance imaging has been developed as a useful imaging modality in the evaluation of the athlete with shoulder pain. Magnetic resonance (MR) imaging is an excellent non-invasive imaging tool that can complement the physical examination in the evaluation of sports-related injuries of the shoulder. The superb soft tissue contrast and multi-planar capabilities of MR imaging make it ideally suitable to provide a global assessment of the soft tissue and osseous structures of the shoulder joint (4).

Table 1 The frequency and percentage of athletics and non athletics.

Lesions	Type of patient	
	Athletic	Non athletic
Bankart	19	13
Osseous Bankart	2	0
Reversed Bankart	2	0
Bankart variants	4	4
RCT[a]	1	7
MDI[a]	4	1
SLAP[a]	3	0
Frequency	35	25
Percentage	58.3	41.7

[a] Abbreviations: SLAP, Superior Labrum Anterior Posterior; RCT, Rotator Cuff Tendon; MDI, Multidirectional Instability.

Table 2 The frequency of pathological appearance of the anterior/inferior labrum on conventional MRI for both groups.

	Frequency	
	Athlete	Non athlete
Anterior/inferior labrum		
NAD[a]	20	19
Clumped	3	1
Torn	12	5
Total	35	25
Posterior labrum		
NAD[a]	34	25
Attenuated	1	0
Total	35	25

[a] Abbreviation: NAD, No Abnormalities Detected.

Table 3 The frequency and percentage of pathological appearance of the inferior labrum on conventional MRI.

RCT[a] lesions	Frequency	
	Athlete	Non athlete
SST[a]:tendinopathy	0	9
Partial tear	0	1
IST[a]	0	1
LHB[a]	0	1
Total	0/35	12/25

[a] Abbreviations: RCT, Rotator Cuff Tendon; SST, Supraspinatous Tendon; IST, Infraspintous Tendon; LHB, Long Head of Biceps.

Conventional MR imaging is usually adequate for the evaluation of patients with suspected rotator cuff disease and the clinical syndrome of impingement. However, in those patients with glenohumeral instability and suspected labral abnormalities, the use of intra-articular gadolinium (direct MR arthrography) will improve the diagnostic accuracy in the detection of subtle labral lesions. The anatomical configuration of a shallow glenoid fossa, combined with the large articular surface of the humeral head, allows for tremendous range of motion of the glenohumeral joint; however, this same anatomical configuration also results in an inherently unstable joint. The capsular structures and the glenoid labrum are static stabilizers that, when combined with the active stabilizing forces of the rotator cuff and long head of the biceps tendon, improve the

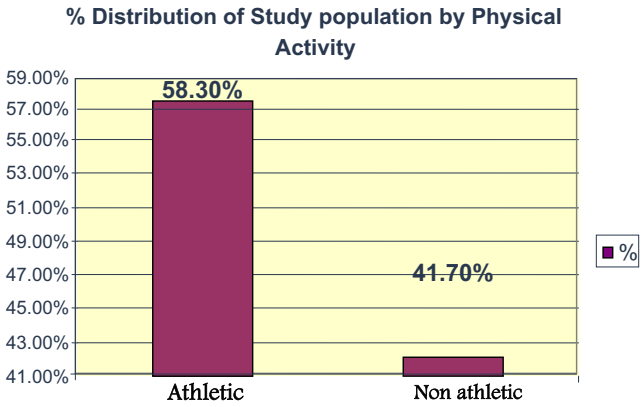

Chart 1 The percentage of distribution of study population according to the physical activity representing athletics (58.3%) versus non-athletics (41.7%) in the study group.

Table 4 The frequency of the pathological lesions of the rotator cuff tendons on direct MRA[a] at the non-athelete group.

RCT[a] lesions	Frequency
SST[a] tendinopathy	4
SST[a] Partial tear	2
SST[a] full thickness tear	2
SST[a] calcific tendinitis	1
SST[a] NAD[a]	1
IST[a] Partial tear	1
Rupture LHB[a]	1
Total	12/25

[a] Abbreviations: NAD, No Abnormalities Detected; RCT, Rotator Cuff Tendon; SST, Supraspinatous Tendon; IST, Infraspintous Tendon; LHB, Long Head of Biceps; MRA, Magnetic Resonance Arthrography.

Table 5 The frequency of different pathological appearance of the anterior/inferior labral injury and its associations as well as posterior labrum pathology on MRA study in both groups.

	Frequency	
	Athlete	Non athlete
Anterior/inferior labrum		
NAD[a]	10	19
Clumped	4	1
Detached	12	5
Detached non-displaced	4	0
+ articular cartilage injury	1	0
+ glenoid fracture	2	0
+ loose bodies	2	0
Total	35	25
Posterior labrum		
NAD[a]	33	25
Torn	2	0
Total	35	25

[a] Abbreviation: NAD, No Abnormalities Detected.

Table 6 Comparative study of the radiological versus the arthroscopic diagnoses in 60 patients.

Final radiological diagnosis MR techniques (MRI[a] ± MRA[a])	Frequency	Arthroscopic diagnosis	Frequency
Bankart	32	Bankart	32
Osseous Bankart	2	Osseous Bankart	2
Reversed Bankart	2	Reversed Bankart	2
Perthes	2	Perthes	2
ALPSA[a]	1	ALPSA[a]	1
GLAD[a]	1	GLAD[a]	1
SLAP[a] lesion	3	SLAP[a] lesion	4
MDI	4	MDI	4
Normal	5	Normal	4
RCT[a] pathology	8	RCT[a] pathology	8
Total	60	Total	60

[a] Abbreviations: ALPSA, Anterior Labrum Periosteal Sleeve Avulsion; GLAD, Glenoid Labrum Articular Disruption; SLAP , Superior Labrum Anterior Posterior; RCT , Rotator Cuff Tendon; MRI, Magnetic Resonance Imaging; MRA, Magnetic Resonance Arthrography.

stability of the glenohumeral joint. Knowledge of the normal MR appearance of the capsule and labrum, along with an understanding of the major anatomical variations, is important in accurately assessing these structures on MR imaging. Multiple studies that demonstrate sensitivities ranging from 78% to 93% and specificities ranging from 68% to 87% for the detection of labral abnormalities using conventional MR imaging have been performed. The use of direct MR arthrography, however, has been shown to increase sensitivities and specificities to the range of 91–93% respectively (5).

The purpose of this study was to assess the diagnostic value of direct MR arthrography compared to conventional MR imaging in the diagnosis of different pathologic entities affecting the capsule-labral complex in athletes and non-athletic population.

In our study, we concluded that the athletes were more subjected to have SLAP lesions (three patients), MDI (four patients), Bankart lesion (19 patients), osseous Bankart (two patients), and Bankart's variants (four patients) more than non-athletic population.

This agreed with (4,5), who compared findings of a group of athletes with age matched non-athletes patients and concluded that SLAP (6/20) and labral injuries were more common in the athlete group compared to the non-athlete group where only two patients show SLAP lesion (2/50) and agreed with (1) where, it stated that traumatic injuries leading to SLAP tears include falls with the arm elevation or forceful elevation and abduction of the arm in the overhead position. In some instances, recurrent shoulder instability episodes can propagate anterior or even posterior labral tears around the glenoid superiorly leading to the SLAP tears.

Conventional MR imaging allows direct visualization of major anatomic structures; yet, its deficiency in depicting lesions associated with glenohumeral instability has led to the increasing use of arthrographic techniques (7).

Comparing conventional MR imaging with MR arthrography concluded that the accuracy of diagnoses can be improved with the addition of an intra-articular injection (8).

In our study, on applying direct intra-articular injection of contrast to distend the joint capsule and to improve the evaluation of smaller intra-articular structures such as the glenoid labrum and glenohumeral ligaments using fluoroscopically guided anterior approach as applied with (5–8,9); Most of these articles had shown superior sensitivity and accuracy of direct MR arthrography over conventional MR imaging, particularly for labral lesions and partial tears of the rotator cuff muscles.

In the present study, on conventional MRI definitive tear of the anteroinferior labrum was diagnosed in twelve patients, while on MRA anterior labral tear appeared in 25 patients. The MRA results were confirmed with arthroscopic findings. When these results were compared with the results of arthroscope, it showed that regarding the antero-inferior labral lesion, the sensitivity of un-enhanced MRI was 72% and specificity 78% while MR arthrography had one false-negative result (sensitivity 95%) and no false-positive results (specificity 100%). Positive predictive value between MRA and arthroscope was 100% and negative predictive value was 21%.

This agreed with (6,8,10), where a retrospective study compared direct MR arthrography with non-enhanced MR imaging of the shoulder in 20 consecutive patients with shoulder instability. Eleven out of 20 patients had additional positive findings on direct MR arthrography but not on non-enhanced MR imaging. (The MRA results were confirmed by arthroscopy.)

In the population group of sport related shoulder injuries, (5,11) found that non-enhanced MR imaging missed two of five anterior labral tears and two of ten SLAP tears that were present on direct MR arthrography.

This also agreed with (8,12), whose results showed the same specificity (100%) as in our study while, the sensitivity of MR arthrography in detecting antero-inferior labral-ligamentous lesions in their study was less than that in ours, and it was 92.8% (26 out of 28 lesions confirmed by arthroscopy).

This agreed with (6,7), where their study showed MR arthrography sensitivity ranged from 79% to 83%, but disagreed with Jbara (13) regarding specificity which ranged from 67% to 85% as our study showed higher specificity (100%).

Our study results regarding specificity also agreed with (16) which stated that MR arthrography showed a sensitivity of 96% and a specificity of 80% for the overall detection of antero-inferior labrum abnormalities. The diagnostic accuracy was 95%.

The results of the Oh et al. study (13) showed MRA sensitivity and specificity of 88% and 96% respectively for anterior labral lesions which conform to our results.

In the present study, posterior labral tears were diagnosed where the criteria used to diagnose were as follows: when the labrum appeared attenuated, detached, displaced, or fragmented. Associated with mild posterior translation of the humeral head was confirmed when the center of the humeral head is posterior to the scapular body line segment by at least 1 mm distance.

This agreed with (14,18) where they used the same criteria to diagnose the posterior labral tears in post-traumatic posterior shoulder dislocation.

On conventional MRI, our study showed normal findings in five patients; however, on MRA, findings of MDI were defined. In the present study, Multidirectional instability (MDI) of the shoulder has been defined as instability in either

two or three directions. The most important features of MDI were described as patients have uncontrolled and involuntary inferior subluxation or dislocation associated with anterior and posterior dislocations, or subluxations of the shoulder.

For the diagnosis, it depends on the rotator interval measurement as well as the capsular distension measurements. The rotator interval capsule was measured on sagittal oblique T1-weighted images with fat saturation. The SOI line was defined as the line from the superior pole (S) of the glenoid through the center of the glenoid (O) to the inferior pole (I) of the glenoid fossa. The anteroinferior dimension (OA) was the maximal capsular dimension perpendicular to the SOI line. The posteroinferior dimension (OB) was the maximal capsular dimension parallel to the SOI line. The anterior (OC), inferior (OD), and posterior (OE) dimensions of the glenohumeral joint capsule were defined as the maximum capsular dimension at 3 o'clock, 6 o'clock, and 9 o'clock, respectively.

This totally agreed with (23,24), where they used the same methods of assessment of rotator interval region as well as the capsular distension to diagnose the MDI patients.

On MRA, the capsular attachment was evaluated in 60 patients; it was found torn in fifteen patients, type III capsular attachment in seven patients, type II in twelve patients and type I in twelve patients. Compared to arthroscopic results it showed 100% specificity.

This agreed with (12,25), and their study confirmed the advantages of MRA in distension of the capsule and distinction of pathologic conditions with 100% specificity.

MRI and MRA showed also supraspinatus tendon tears (partial and complete tears) in two (out of three) patients. The MRA results were confirmed by arthroscopy. A possible explanation for these tears may be extreme tension sustained by the supraspinatus tendon at the time of posterior humeral dislocation.

This agreed with (5) as well as (16) where on MRA, they reported that posterior labral tears are less common than anterior labral tears in their studies. However, they also detected associated rotator cuff tears in the form of full thickness tear of supraspinatus tendon. Their findings were confirmed by arthroscope as well.

The current study observed associated lesions of the superior labrum in shoulder instability where on MRI one patient showed type I SLAP lesion while on MRA; besides the patient showing type I SLAP lesion, two more patients showed type II which were missed by MRI. This was confirmed with the results of the arthroscope, proving that MRA is more sensitive than conventional MRI in diagnosing SLAP lesions.

The ALPSA lesions were misinterpreted as normal labrum in four patients in MRA study; this may be attributed to the healed antero-inferior labrum at antero-medial position at the scapular neck.

Our study agreed with (1,20) study where they performed conventional MRI followed by MRA for six patients with SLAP lesions (arthroscopy diagnosed). MRI diagnosed only one of the six while MRA diagnosed four out of the six patients. They reported that associated SLAP type II seems to be more common with shoulder instability. This was diagnosed with MRA and confirmed with arthroscope.

Finally, in the present study, the sensitivity of un-enhanced MRI was 72%, and specificity 78%, while MR arthrography showed sensitivity of 78%, and specificity of 100%. Positive predictive value between MRA and arthroscope was 100%.

5. Conclusion

We believe that direct MR arthrographic imaging is well suited for detecting intra-articular lesions of the shoulder joint in the athletic and non-athletic populations. The capsulolabral and ligamentous injuries are more common in the athletic group while the non-athletic population are more prone to rotator cuff tendons injury. The presented diagnostic results of MR arthrography are superior to the results of un-enhanced MRI. So, Direct MR arthrography can act as a reliable diagnostic tool prior to surgical or arthroscopic intervention.

MR techniques cannot replace arthroscopy; however, they could be a potent additional tool for diagnosis of the main pathological affection of the shoulder joint guided by the type of the population, which proved to have good impact on the diagnosis. It can help to reduce arthroscopic interventions for purely diagnostic purposes and without any therapeutic consequences.

Conflict of interest

The authors declare that they have no conflict of interest.

References

(1) Daniel J. Solomon, William N. Levine: SLAP tears: pearls and pitfalls in diagnosis and management. Sports medicine update; January/February 2011.
(2) Al Hiari A. Shoulder Instability: the role of MR arthrography in diagnosing antero-inferior labroligamentous lesions our experience at King Hussein Medical Center. Pak J Med 2008;2008(24), 16–11.
(3) Magee Thomas. 3-T MRI of the shoulder: is MR arthrography necessary? AJR Am J Roentgenol 2009;192:86–9.
(4) Cerynik DL, Ewald TJ, Sastry A, Amin NH, Liao JG, Tom JA. Outcomes of isolated glenoid labral injuries in professional baseball pitchers. Clin J Sport Med 2008;18(3):255–8.
(5) Jarraya Mohamed, Roemer Frank W, Gale Heather I, Landreau Philippe, D'Hooghe Pieter, Guermazi Ali. MR-arthrography and CT-arthrography in sports-related glenolabral injuries: a matched descriptive illustration. Insights Imaging. Springerlink: Published online; 2016.
(6) Jbara Marlena, Qichen, Marten Paul, Morcos Morcos, Beltran Javier. Shoulder MR arthrography: how, why, when. Radiol Clin N Am 2005;43:683–92.
(7) Ricchetti Eric T, Ciccotti Michael C, Ciccotti Michael G, Williams Jr Gerald R, Lazarus Mark D. Sensitivity of preoperative magnetic resonance imaging and magnetic resonance arthrography in detection of panlabral tears of the glenohumeral joint. Arthrosc: J Arthrosc Relat Surg 2013;29(2):274–9.
(8) Agha Mahmoud, Gamal Nasser. MR arthrogram for shoulder microinstability and hidden lesions. Alex J Med 2015;51 (3):185–90.
(9) Fotiadou Anastasia, Drevelegas Antonios, Nasuto Michelangelo, Guglielmi Giuseppe. Diagnostic performance of magnetic resonance arthrography of the shoulder in the evaluation of anteroinferior labrum abnormalities: a prospective study. Insights Imaging 2013;4:157–62.
(10) Liavaag S, Stiris MG, Svenningsen S, Enger M, Pripp AH, Brox JI. Capsular lesions with glenohumeral ligament injuries in patients with primary shoulder dislocation: magnetic resonance imaging and magnetic resonance arthrography evaluation. Scand J Med Sci Sports 2011;21:e291–7.

(11) Lecouvet Fredreic E, Simoni Paolo, Koutaïssoff Sophi, Bruno C, Berg Vande, Malghem Jacques, et al. Multidetector Spiral CT arthrography of the shoulder. Clinical applications and limits, with MR arthrography and arthroscopic correlations. Eur J Radiol 2008;68:120–36.
(12) Hiari Asem Al. Shoulder instability: the role of MR arthrography in diagnosing antero-inferior labroligamentous lesions our experience at King Hussein Medical Center. Pak J Med Sci January–March 2008;24(1):6–11.
(13) Oh DK, Yoon YC, Kwon JW, Choi SH, Jung JY, Bae S. Comparison of indirect isotropic MR arthrography and conventional MR arthrography of labral lesions and rotator cuff tears: a prospective study. AJR Am J Roentgenol 2009;192(2):473–9.
(14) Saupe Nadja, White Lawrence M, Bleakney Robert, Schweitzer Mark E, Recht Michael P, Jost Bernhard, et al. Acute traumatic posterior shoulder dislocation: MR findings. Radiology 2008;248:185–93, July.
(16) Schoenfeld AJ, Lippitt SB. Rotator cuff tear associated with a posterior dislocation of the shoulder in a young adult: a case report and literature review. J Orthop Trauma 2007;21:150–2.
(18) Mohamed Safaa Aboelkaseem, Ebied Osama Mohamed, Abdullah Mohamed Shawky, Mohamed Hala Hafez, Elmowafy Hesham Mohamed Zaky. The value of MRI in evaluation of shoulder pain. Int J Med Imag 2014;2(4):83–9.
(20) Khan Ali Nawaz, Desai Niranjan, Rudralingam Velauthan, Shoulder Sirhan Alvi. Glenoid labrum injury MRI: eMedicine radiology. Musculoskeletal 2009.
(21) Pavic Roman, Margetic Petra, Bensic Mirta, Brnadic Renata Letica. Diagnostic value of US, MR and MR arthrography in shoulder instability. Injury Int J Care Injured 2013;44(S3):S26–32.
(22) Doshi R, Maheshwari S, Singh J. Review article: MR anatomy of normal shoulder. Ind J Radiol Imaging 2002;12(2):261–6.
(23) Jacobson Jon A, Lin John, Jamadar David A, Hayes Curtis W. Aids to successful shoulder arthrography performed with a fluoroscopical guided. Anterior Approach Radiogr 2003;23:373–8.
(24) Lee Hui Jin, Kim Na Ra, Moon Sung Gyu, Ko Sung Min, Park Jin-Young. Multidirectional instability of the shoulder: rotator interval dimension and capsular laxity evaluation using MR arthrography. Skeletal Radiol 2013;42:231–8.
(25) Provencher Matthew T, Dewing Christopher B, Bell Josh, McCormick Frank, Solomon Daniel J, Rooney Timothy B, et al. An analysis of the rotator interval in patients with anterior, posterior, and multidirectional shoulder instability. Arthrosc: J Arthrosc Relat Surg 2008;24(8):921–9.